Support Information

Superhydrophobic, biocompatible MXene-based multifunctional E-textiles for wireless transmission system, electromagnetic interference shielding and healthcare monitoring

Junshu Feng,[ab] Zhenhua Tang,*[ab] Guo-Xun Zeng,[c] Tingsu Liu,[ab] Long Ye,[ab] Xin-Gui Tang,[ab] Yan-Ping Jiang[ab] and Xiu-Juan Jiang[d]

[a]School of Physics and Optoelectric Engineering, Guangdong University of Technology, Guangzhou Higher Education Mega Center, Guangzhou, 510006, China
E-mail: tangzh@gdut.edu.cn

[b]Guangdong Provincial Key Laboratory of Sensing Physics and System Integration Applications, Guangzhou, Guangdong 510006, China

[c]School of Materials and Energy, Guangdong University of Technology, Guangzhou Higher Education Mega Center, Guangzhou, Guangdong 510006, China

[d]School of Mechanical and Electrical Engineering, Guangdong University of Technology, Guangzhou Higher Education Mega Center, Guangzhou, Guangdong 510006. China

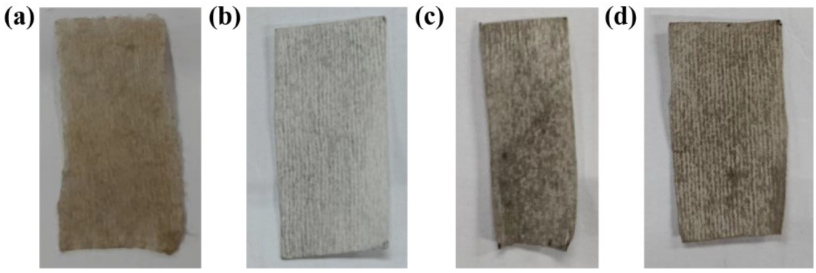

Figure S1. AP was treated with PDA (a) ultrasonic homogenizer for 10 minutes, (b) room temperature soaking for 3 hours, (c) room temperature soaking for 7 hours, and (d) room temperature soaking for 24 hours, respectively.

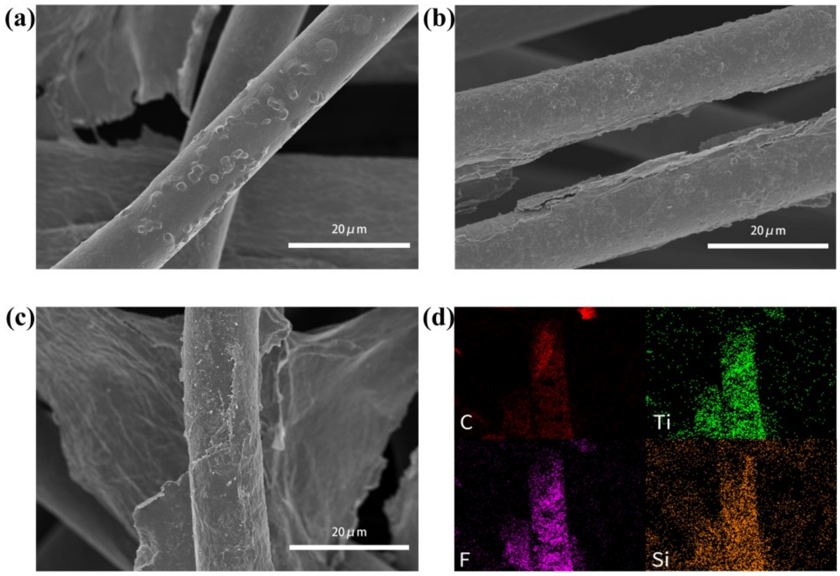

Figure S2. (a) APM-1AF, (b) APM-6AF, (c) APM-9AF scanning electron microscopy images and corresponding (d) EDS elemental map images of C, Ti, F, Si.

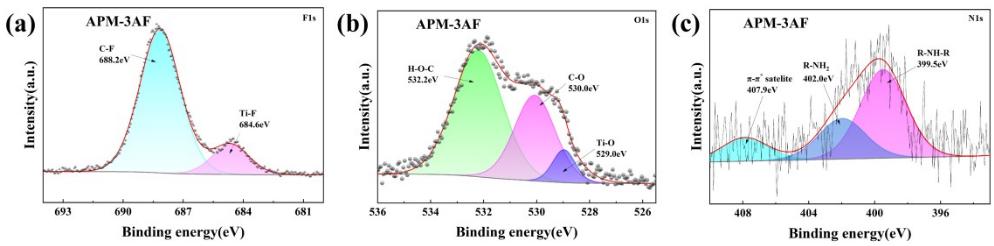

Figure S3. XPS spectra of (a) F1s, (b) O1s, and (c) N1s of the APM-3AF sample.

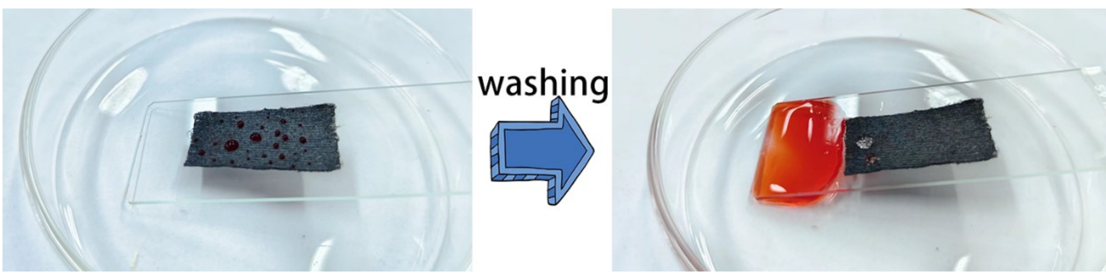

Figure S4. Self-cleaning ability of APM-3AF sample.

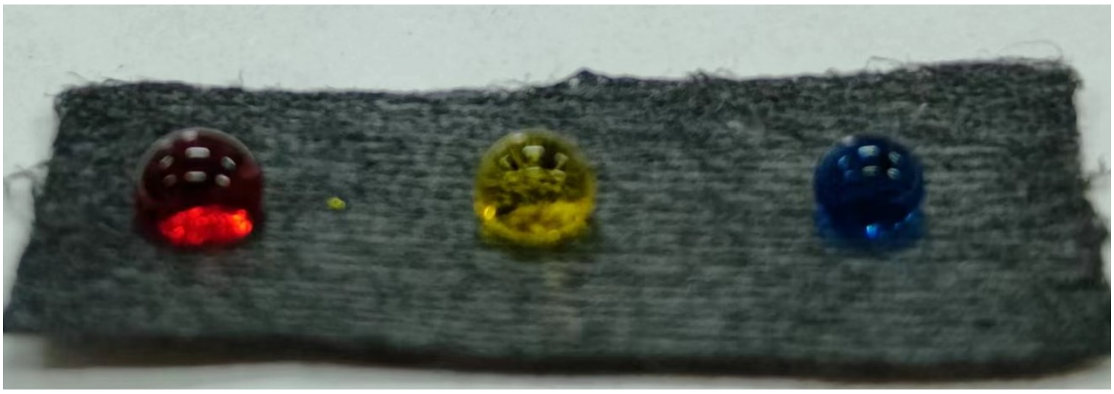

Figure 5. Photos of water droplets with different pH values (left HCL, pH=1, middle deionized water, pH=7, right KOH, pH=13) on the APM-3AF sample.

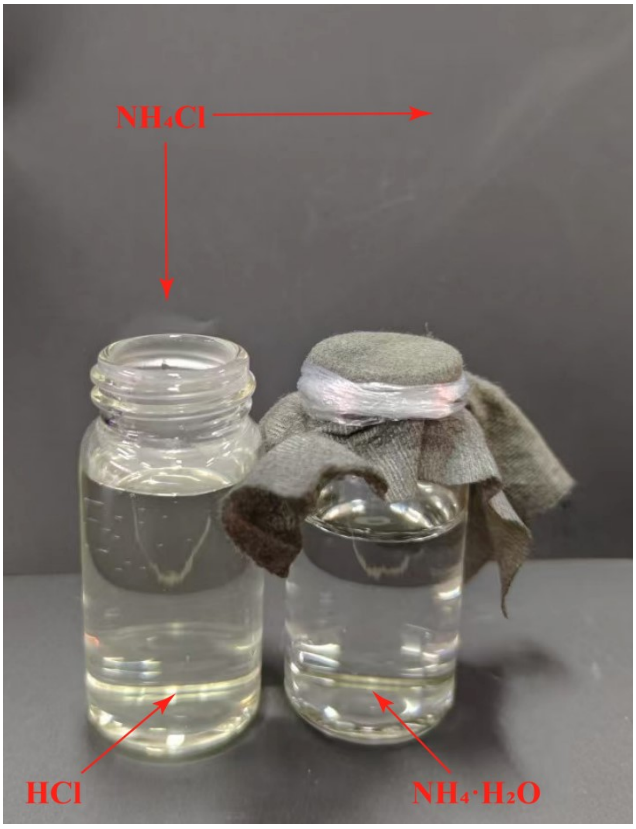

Figure S6. Photo of ammonia escaping from a small bottle covered with APM-3AF textile and reacting with dilute hydrochloric acid.

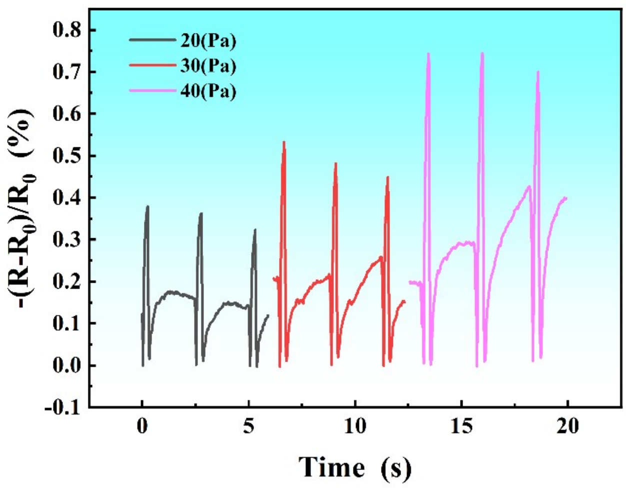

Figure 7. Resistance response of samples under extremely low pressure.

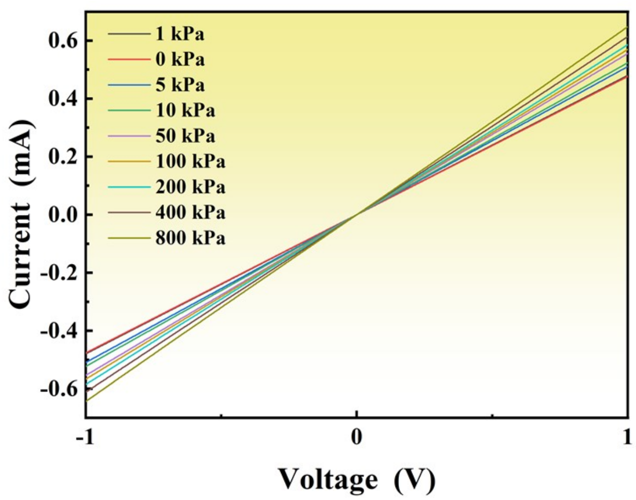

Figure S8. Current voltage curves of APM-6AF sensor under different pressures.

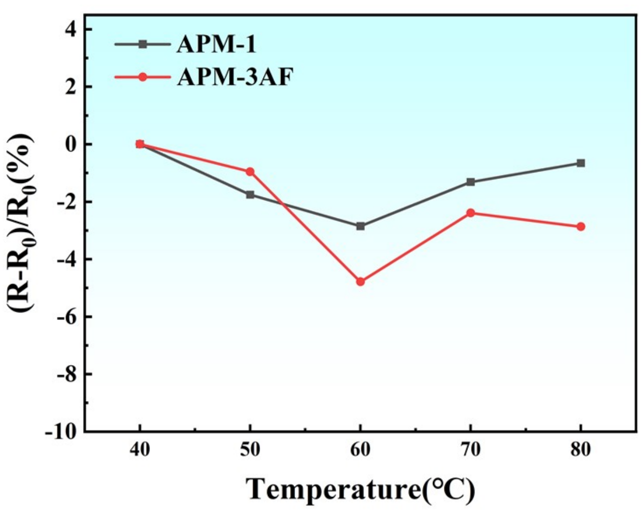

Figure S9. Relative changes in resistance of APM-1 and APM-3AF at different temperatures.

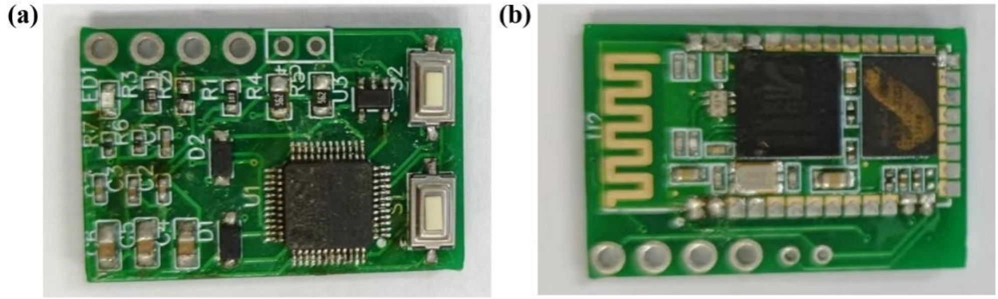

Figure S10. (a) shows the acquisition module and ADC module using STM32F103C8T6 as the central processor. (b) HC-05 Bluetooth module.

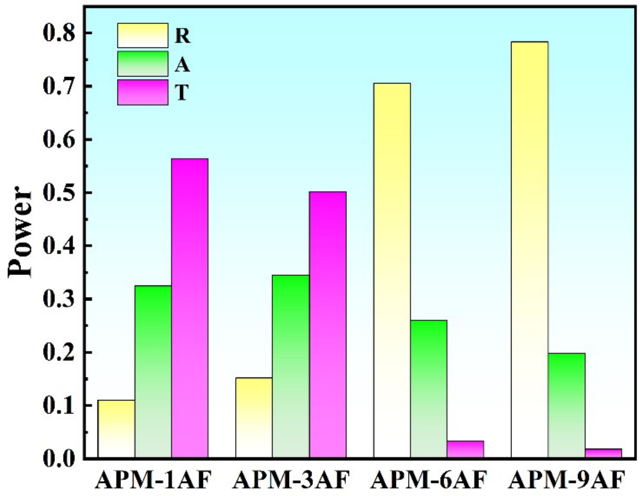

Figure S11. R, A and T of APM-XAF (X = 1,3,6,9).

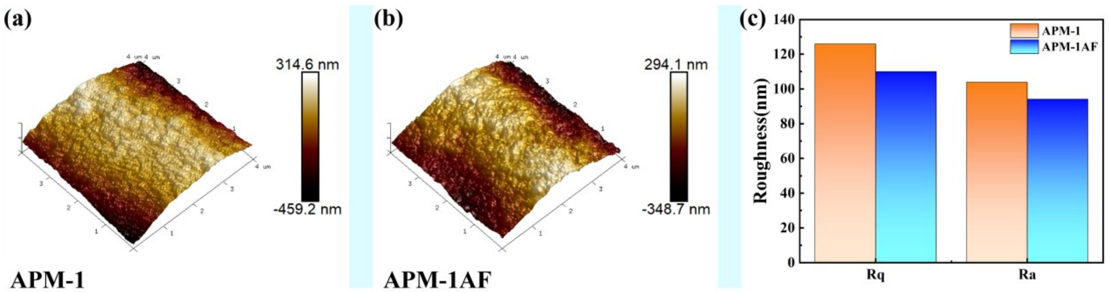

Figure S12. Three-dimensional morphology map of (a) APM-1 surface and (b) APM-1AF surface. (c) Surface roughness distribution of APM-1 and APM-1AF.

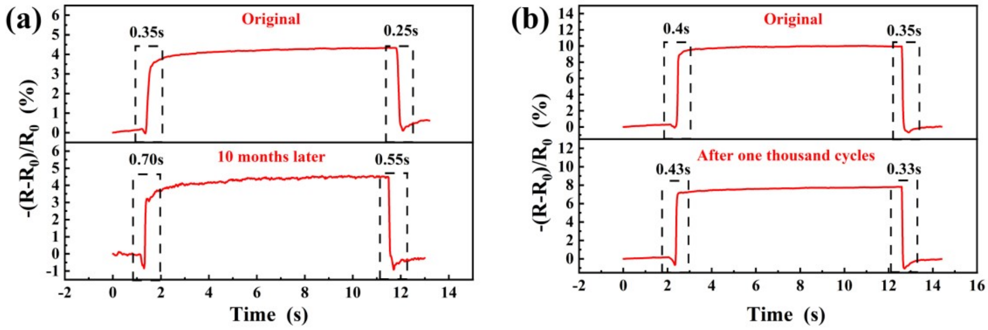

Figure S13. (a) Comparison of changes in reaction time of AFM-1AF after ten months. (b) Comparison of changes in sample reaction time after one thousand cycles.

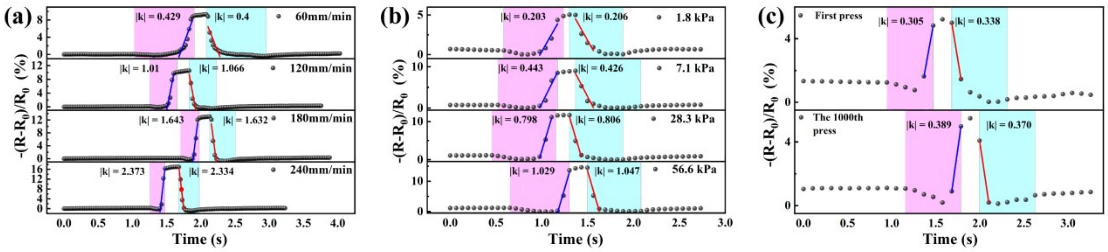

Figure S14. The rate of resistance change of the sample was compared under (a) different loading and unloading rates, (b) different pressures, and (c) after 1000 loading-unloading cycles.

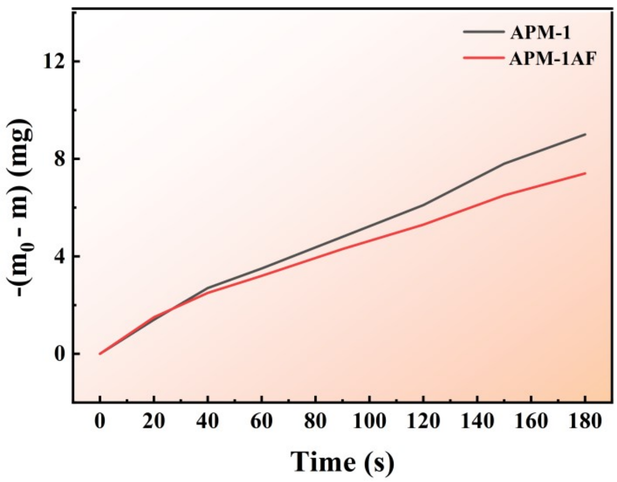

Figure S15. The amount of water vapor at 80 °C evaporated through the 1.5 cm diameter sample bottle neck sealed by (a) APM-1 and (b) APM-1AF within a certain period of time.

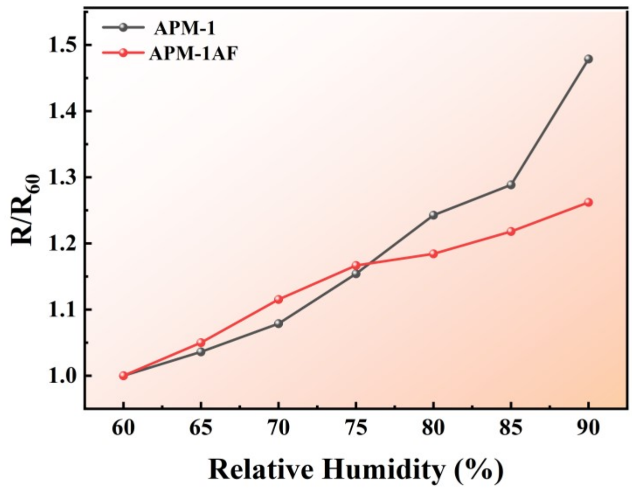

Figure S16. The resistance changes generated by (a) APM-1 and (b) APM-1AF with varying relative humidity.

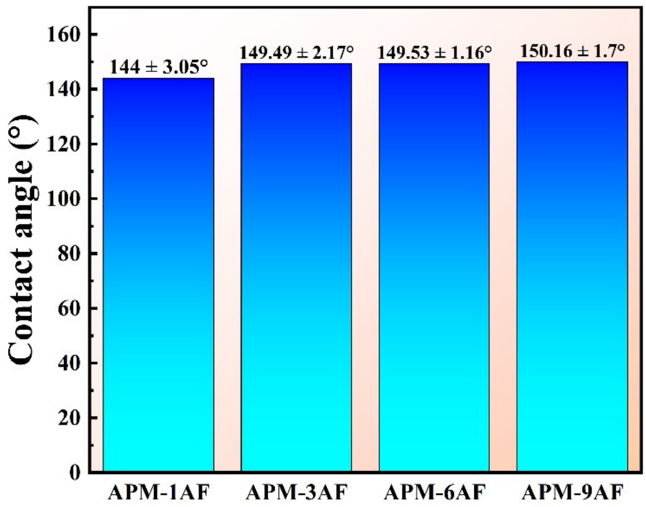

Figure S17. The water contact angle error bars of APM-XAF (X = 1, 3, 6, 9).

2d2a4b468c868
dfbfeda04563be7

Video S1. Wireless transmission system testing finger bending video.

5d2f59abbec28b
e0cd185cf89f6d4

Video S2. Testing electromagnetic interference shielding using waveguide method.

Table S1. The performance comparisons of the APM-XAF with other e-textiles in previous reports.

Materials	*GF (kPa^{-1}) (in small pressure)*	*Hydrophobic performance*	*Electromagnetic interference shielding*	*Ref.*
SBS/AGNW/PU	0.2	NO	NO	[1]
Cot@PDA/MXene/PF	1.4	hydrophobicity	32dB	[2]
Suede@PDA/C-MWCNT	0.46	Superhydrophobicity	NO	[3]
PDMS/MXene AP-X	0.24	NO	>30dB	[4]
bark-shaped MXene/textiles (BMFs)	28.7	NO	35.2dB	[5]
MXene/AgNW silk		Superhydrophobicity	42dB	[6]
HDTMS-PPy/MXene cotton fabric	0.6	Superhydrophobicity	NO	[7]
Cu3Se2/CC	0.34	NO	63.3dB	[8]
CC@FeCo/MXene/PDMS	0.17	NO	45.5dB	[9]
Silicone/MXene AP	1.62	hydrophobicity	NO	[10]
APM-XAF	0.56	Superhydrophobicity	17dB	This work

References

[1] S. Chen, S. Liu, P. Wang, H. Liu and L. Liu, *J. Mater. Sci.*, 2018, **53**, 2995-3005.

[2] T. Zhang, B. Song, X. Li, K. Yang, J. Yang, G. Tian, J. Ma, *ACS Appl. Polym. Mater.*, 2023, **5**, 6296-6306.

[3] X. Sun, Q. Wang, J. Zhan, T. Yang, Y. Zhao, C. Sun, M. Aisha, M. Guo, S. Tang, H. Zhao, L. Wang and J. Liu, *ACS Appl. Nano Mater.*, 2023, **6**, 10746-57.

[4] D. Yao, Z. Tang, Z. Liang, L. Zhang, Q. Sun , J. Fan , G. Zhong, Q. Liu, Y. Jiang, X. Tang, V. A. L. Roy and J. Ouyang, *J. Colloid Interface Sci.*, 2023, **630**, 23-33.

[5] X. Zheng, P Wang, X. Zhang, Q. Hu, Z. Wang, W. Nie, L. Zou, C. Li and X. Han, *Compos. Pt. A-Appl. Sci. Manuf.*, 2022, **152**, 106700.

[6] L. Liu, W. Chen, H. Zhang, Q. Wang, F. Guan and Z Yu, *Adv. Funct. Mater.*, 2019, **29**, 1905197.

[7] J. He, F. Shi, Q. Liu, Y. Pang, D. He, W. Sun, L. Peng, J. Yang, M. Qu, *Colloid Surf. A-Physicochem. Eng. Asp.*, 2022, **642**, 128676.

[8] P. Zong, M. Chen, X. Wang, H. Liu, Z. He, Y. Ou, and C. Sun, *Carbon.*, 2025, **232**, 119814.

[9] S. Wang, D. Li, L. Jiang and D. Fang, *Compos. Sci. Technol.*, 2022, **221**, 109337.

[10] C. Ma, Q. Yuan, H. Du, M. Ma, C. Si and P. Wan, *ACS Appl. Mater. Interfaces*, 2020, **12**, 34226-34.